

1 **A Global Inventory of Small Floating Plastic Debris**

2 Erik van Sebille<sup>1,2</sup>, Chris Wilcox<sup>3</sup>, Laurent Lebreton<sup>4</sup>, Nikolai Maximenko<sup>5</sup>, Britta  
3 Denise Hardesty<sup>3</sup>, Jan A. van Franeker<sup>6</sup>, Marcus Eriksen<sup>7</sup>, David Siegel<sup>8</sup>, Francois  
4 Galgani<sup>9</sup>, and Kara Lavender Law<sup>10</sup>

5 <sup>1</sup> Grantham Institute & Department of Physics, Imperial College London, London,  
6 United Kingdom

7 <sup>2</sup> ARC Centre of Excellence for Climate System Science, Climate Change Research  
8 Centre, University of New South Wales, Sydney, Australia

9 <sup>3</sup> CSIRO Oceans and Atmosphere Flagship, Hobart, Tasmania, Australia

10 <sup>4</sup> Dumpark Data Science, Wellington, New Zealand

11 <sup>5</sup> International Pacific Research Center, School of Ocean and Earth Science and  
12 Technology, University of Hawai'i at Mānoa, Honolulu, Hawaii, USA

13 <sup>6</sup> IMARES, Wageningen-UR, Den Burg (Texel), Netherlands

14 <sup>7</sup> Five Gyres Institute, Los Angeles, California, USA

15 <sup>8</sup> Department of Geography and Earth Research Institute, University of  
16 California, Santa Barbara, CA, USA

17 <sup>9</sup> Institut Français de Recherche pour l'Exploitation de la Mer (IFREMER), Bastia,  
18 France

19 <sup>10</sup> Sea Education Association, Woods Hole, Massachusetts, USA

20 **Abstract**

21 Microplastic debris floating at the ocean surface can harm marine life.  
22 Understanding the severity of this harm requires knowledge of plastic  
23 abundance and distributions. Dozens of expeditions measuring microplastics  
24 have been carried out since the 1970s, but they have primarily focused on the  
25 North Atlantic and North Pacific accumulation zones, with much sparser  
26 coverage elsewhere. Here, we use the largest dataset of microplastic  
27 measurements assembled to date to assess the confidence we can have in global  
28 estimates of microplastic abundance and mass. We use a rigorous statistical  
29 framework to standardize a global dataset of plastic marine debris measured  
30 using surface-trawling plankton nets and coupled this with three different ocean  
31 circulation models to spatially interpolate the observations. Our estimates show  
32 that the accumulated number of microplastic particles in 2014 ranges from 15 to  
33 51 trillion particles, weighing between 93 and 236 thousand metric tons, which  
34 is only approximately 1% of global plastic waste estimated to enter the ocean in  
35 the year 2010. These estimates are larger than previous global estimates, but  
36 vary widely because the scarcity of data in most of the world ocean, differences  
37 in model formulations, and fundamental knowledge gaps in the sources,  
38 transformations and fates of microplastics in the ocean.

39 **1. Introduction**

40 Plastic debris has been documented in all marine environments, from coastlines  
41 to the open ocean (Barnes *et al* 2009), from the sea surface to the sea floor  
42 (Schlining *et al* 2013), in deep-sea sediments (Woodall *et al* 2014) and even in  
43 Arctic sea ice (Obbard *et al* 2014). The best-measured reservoir of plastic marine

44 debris on a global scale is that of buoyant plastics floating at the sea surface. Yet  
45 observational data, even in the extensively surveyed western North Atlantic  
46 Ocean (Law *et al* 2010) and eastern North Pacific Ocean (e.g. Goldstein *et al*  
47 2012, Law *et al* 2014), have not yet determined the full extent of large  
48 accumulations of debris associated with the converging surface currents in  
49 ocean subtropical gyres. In the southern hemisphere gyres there are scarcely  
50 enough data to confirm the presence of floating plastic debris (Eriksen *et al*  
51 2013, Cózar *et al* 2014, Eriksen *et al* 2014), and the vast majority of the sea  
52 surface outside the gyres remains unsurveyed, introducing potentially large  
53 errors in global estimates of the amount of floating plastic.

54 Little is known about the transformations of plastics in seawater, including the  
55 time scales of degradation and its ultimate sinks. Weakened by UV radiation,  
56 chemical degradation, wave mechanics and grazing by marine life, plastics  
57 fragment into smaller and smaller pieces; plastic particles smaller than 5 mm in  
58 size are commonly referred to as microplastics. It has been suggested that plastic  
59 never fully degrades, yet expected increases in plastic concentration in response  
60 to increased production and use have not been consistently observed (e.g.  
61 Thompson *et al* 2004, Law *et al* 2010), and global budgeting exercises find less  
62 material on the ocean surface than expected (Cózar *et al* 2014, Eriksen *et al*  
63 2014). To properly evaluate the risk of plastic contamination to marine  
64 organisms, understanding the amount, form and distribution of plastic in the  
65 marine environment, and how these evolve in time, is necessary. In this study,  
66 we focus on assessing the amount and distribution of 'small' (nominally <  
67 200 mm) plastic debris on the ocean surface, as these are by far the most

68 sampled data set and also have demonstrated biological impact (Rochman *et al*  
69 2015), although larger items can also impact biota.

70 At the sea surface, microplastic marine debris is typically measured by surface-  
71 towing plankton nets with mesh ranging from 0.1 to 0.5 mm, which capture  
72 particles limited to the size of the net aperture. Net tow sampling efforts  
73 typically capture plastic particles smaller than 10 mm in size (Morét-Ferguson *et*  
74 *al* 2010), while less numerous larger items are observed by visual surveys with  
75 ships or aircraft. The vast majority of observations since the 1970s have been  
76 made using plankton nets, with broadly similar sampling methodologies but  
77 variable reporting units (particle count per area or volume, or mass per area or  
78 volume). In contrast, visual surveys of macroplastic debris are conducted using a  
79 wide range of survey protocols ranging from (non-quantitative) opportunistic  
80 sightings to rigorous distance sampling methods (e.g. Williams *et al* 2011) for  
81 which it is difficult to satisfy all underlying methodological assumptions  
82 (Buckland *et al* 2001). In addition to the difficulty in reconciling different visual  
83 survey techniques (although useful reference standardized approaches based on  
84 distance sampling have been proposed, e.g. Ryan 2013), large debris is less  
85 numerically abundant than microplastics and its drift behavior and  
86 accumulation patterns are likely quite different because of its size, buoyancy and  
87 windage. Even though large debris accounts for a substantial mass of ocean  
88 plastics, for the reasons described above, we consider only data from plankton  
89 net trawls, which primarily collect microplastics in this analysis.

90 With the recent addition of relatively large and more geographically widespread  
91 datasets, and oceanographic numerical models that predict debris accumulation

92 at the sea surface from surface current patterns, the first global estimates of the  
93 reservoir of floating plastic debris have recently been reported (Cózar *et al* 2014,  
94 Eriksen *et al* 2014). Using plankton net data (1,127 trawls) spatially averaged in  
95 accumulation and non-accumulation zones defined from a statistical  
96 oceanographic model (Maximenko *et al* 2012), Cózar *et al* (2014) estimated  
97 between 7,000 and 35,000 tons of floating plastic (0.20 to 100 mm in size) in the  
98 Atlantic, Pacific and Indian Oceans combined. Using a nearly independent  
99 plankton net dataset (680 trawls), Eriksen *et al* (2014) computed a global  
100 estimate of floating plastic (0.33 to 200 mm in size; 66,140 metric tons) using a  
101 different oceanographic model (Lebreton *et al* 2012) whose output was scaled  
102 by the globally measured plastic concentration. Given the methodological  
103 differences between these studies, it is encouraging that the resulting estimates  
104 are so close.

105 Here we estimate the global standing stock of small floating plastic debris with  
106 the most comprehensive dataset, ocean models and ocean plastic input  
107 estimates available. We compiled all available plastic data collected with surface-  
108 trawling plankton nets (more than 11,000 observations, including those in Cózar  
109 *et al* (2014) and Eriksen *et al* (2014)), resolved sampling biases and other  
110 variations using a statistical model, and then used the standardized dataset to  
111 scale the outputs of three ocean circulation models. By comparing the three  
112 scaled model solutions, we assessed where debris patterns are well predicted  
113 and identified regions where discrepancies between solutions must be resolved  
114 through improved process description in models, additional oceanographic data

115 collection and/or increased understanding of sources, composition, and lifecycle  
116 of plastic debris.

117

## 118 **2. Methods**

### 119 *2.1 Plankton surface-trawl dataset*

120 Plankton nets can capture any debris larger than the net mesh and smaller than  
121 the net mouth, but net dimensions vary between studies and maximum particle  
122 size is often not reported. Since most particles collected in plankton nets are  
123 millimeters in size or smaller, from here forward we use the term  
124 “microplastics” not in its strict definition (as particles < 5 mm in size), but  
125 instead to conveniently refer to all plastic debris collected in surface-trawling  
126 plankton nets.

127 There are two relevant measures for net-collected plastic debris: particle count  
128 and mass. Both have their merits. Samples are easier to count than to weigh,  
129 especially while underway at sea, and the number of particles may be more  
130 relevant for an exposure assessment. On the other hand, as a conservative  
131 variable, mass can more easily be related to source estimates, and will  
132 eventually be needed to close the mass balance of ocean plastics. Because of  
133 these considerations, we report both measures.

134 Plastic data collected using surface-trawling plankton nets were identified by  
135 literature search and data were assembled either directly from the publication  
136 or by contacting the corresponding author (Table S1). Additional unpublished

137 data were provided by contributing authors. In total 27 floating debris studies  
138 were identified, with 11,854 surface trawls carried out between 1971 and 2013,  
139 spanning all major ocean basins except the Arctic. Given the long time span over  
140 which samples were collected, we addressed sampling year as a potential bias  
141 when we standardized the data (see section 2.2). Net mesh ranged from 0.15 to  
142 3.0 mm in size, although more than 90% of observations were collected using a  
143 manta net or neuston net with 0.333 or 0.335 mm mesh. Most studies did not  
144 report the maximum size of plastic debris collected. All data reported in units of  
145  $\#/m^3$  were converted to  $\#/m^2$  by multiplying by the submerged height of the  
146 net, and then cast into units of  $\#/km^2$ . Nearly all studies reported plastic  
147 abundance in count units, and two-thirds reported data in mass units. However,  
148 the three largest datasets (comprising 82% of total observations) only reported  
149 counts. Conversions to mass for datasets in which only count was reported were  
150 made using factors derived from empirical data collected in similar geographic  
151 regions, during similar time periods and/or using similar sampling methods  
152 (Table S1).

153 Microplastic abundance at the sea surface has been shown to vary with wind  
154 speed due to vertical mixing (Kukulka *et al* 2012, Reisser *et al* 2015), yet most  
155 studies did not report wind data. To evaluate the relationship between wind  
156 speed and plastic abundance as a source of variability in the data set, we used  
157 daily-averaged wind speed from the ECMWF ERA-Interim global atmospheric  
158 reanalysis (Dee *et al* 2011) interpolated to each surface trawl date and location.  
159 ERA-Interim output is available beginning January 1, 1979; thus, 222 surface  
160 trawls collected prior to 1979 were omitted from our analysis.

## 161 *2.2 Data standardization using statistical modeling*

162 Microplastics sampled were collected in a wide range of conditions over a multi-  
163 decadal period. Before scaling ocean circulation model outputs with these data,  
164 we first removed variability associated with factors that could affect either the  
165 concentration of plastic in the ocean or the representativeness of the samples,  
166 such as sampling year, wind speed, distance of the tow, and others. We used a  
167 generalized additive model (GAM; Wood 2006), implemented in the R statistical  
168 language (R Core Team 2013), to estimate the relationships between these  
169 variables and the observed plastic concentration (in counts), and then used  
170 those relationships to adjust the observations to represent standardized  
171 conditions.

172 We first created a base model using a spherical smooth term (two-dimensional  
173 spline) to represent location on the globe, assuming that repeated samples in the  
174 same location should share an underlying average value. We then explored the  
175 effects of sampling year, wind speed, trawl length, and study ID on measured  
176 plastic concentrations. To account for changes in time we explored  
177 incorporating either a smooth term or first and second order polynomials with  
178 year since 1950, approximately the beginning of commercial plastic production,  
179 to allow for non-linearity in the relationship. We did the same to evaluate the  
180 sampling bias associated with variable wind speed. We used the model residuals  
181 to diagnose any locations of poor fit in the model, in particular those resulting  
182 from discontinuities between sampling regions caused by land. Where we found  
183 these issues, we allowed a transition in the spatial surface by incorporating a  
184 nonlinear function of the distance from the discontinuity as a predictor variable.



185 We defined the set of potential GAMs a priori and used the Akaike information  
186 criterion (AIC; Burnham and Anderson 2002) to determine the best model,  
187 balancing parsimony and fit across the full set of possible models. We chose a  
188 Tweedie distribution with a parameter of 1.6 to allow for over-dispersion in the  
189 data. The best performing GAM was used to predict the plastic concentrations  
190 that would have been observed for each sample had it been taken under no-wind  
191 conditions in the year 2014 (hereafter the “standardized dataset”). We also  
192 estimated the standard error in our predictions based on the variance-  
193 covariance structure among the fitted parameters, using the tools provided in  
194 the mgcv package (Wood 2006). These standard errors were used to estimate  
195 the 95% confidence intervals on the standardized plastic concentrations. Where  
196 calculations required values in mass, as opposed to counts, we used the ratio of  
197 mass to count from the observational data (as originally reported or using the  
198 conversion factors discussed above) to convert standardized counts to  
199 standardized masses.

200

### 201 *2.3 Ocean circulation models*

202 The non-uniformly distributed, standardized plastic concentrations must be  
203 spatially interpolated in order to produce a global map of microplastic  
204 distribution. This is particularly important in regions of low coverage, such as in  
205 the Southern Hemisphere. While in principle this could be done with simple  
206 interpolation methods such as kriging, more realistic results can be obtained by  
207 synthesizing observations with ocean circulation model predictions. In order to  
208 assess the dependence of the resulting global microplastic distribution on the

209 choice of ocean circulation model, we used three largely independent models. As  
210 in Maximenko *et al* (2012), Lebreton *et al* (2012) and Van Sebille *et al* (2012),  
211 we released virtual microplastic in ocean circulation models to obtain maps of  
212 likely distribution of microplastics from transport by ocean surface currents.  
213 Each model-predicted distribution provides one regression parameter per basin.  
214 The results of this regression exercise depend on the assumptions made in each  
215 ocean circulation model, such as how surface currents are derived, how plastic is  
216 released into the ocean, and whether and how microplastics are removed from  
217 the surface.

218 The Maximenko model (Maximenko *et al* 2012) uses a transition matrix  
219 approach, based on the probability of particle travel between  $\frac{1}{2}^\circ$  bins calculated  
220 from trajectories of a historical global set of satellite-tracked drifting buoys  
221 (<http://www.aoml.noaa.gov/phod/dac/index.php>). Microplastics, represented as a virtual tracer,  
222 are advected through the ocean by iterating the transition matrix for 10 years.  
223 As a source function, this model used a uniform distribution of microplastics  
224 over the global ocean. They showed that in 2-3 years a high concentration of  
225 microplastics builds up in the five subtropical gyres, where it creates spatial  
226 patterns not sensitive to the initial condition, and with the potential to persist  
227 for hundreds of years before washing ashore.

228 The Lebreton model (Lebreton *et al* 2012) uses ocean velocity fields from the  
229  $1/12^\circ$  global HYCOM circulation model. Virtual microplastics are sourced on  
230 major river mouths as a function of urban development (impervious surface  
231 area) within individual watershed, on coastlines as a function of coastal  
232 population, and on major shipping routes as a function of shipping traffic. Here,

233 we use the coastal population scenario only, for consistency with the Van Sebille  
234 model (below). Microplastics are continuously released in increasing amounts  
235 based on global plastic production data (Plastinum 2009) and are advected by  
236 the ocean surface velocity field for thirty years.

237 Finally, the Van Sebille model (van Sebille *et al* 2012, van Sebille 2014) also  
238 advects microplastics in ocean currents captured in a transition matrix built  
239 from the trajectories of drifting buoys, as in the Maximenko model. Here, the  
240 source function is assumed to be proportional to the human population within  
241 200 km of the coast, scaled by the amount of plastic waste available to enter the  
242 ocean by country in 2010 (Jambeck *et al* 2015, what they term “mismanaged  
243 waste”). Microplastics are continuously released at each coastal point over 50  
244 years (1964-2014), increasing in time based upon global plastic production data  
245 (Plastics Europe 2013).

246 All three ocean circulation models treat microplastic sinks differently. While the  
247 Lebreton and Van Sebille models have no sinks at all (i.e., all released  
248 microplastic stays in the ocean indefinitely), microplastics in the Maximenko  
249 model can “wash ashore” when they enter grid cells with a model shoreline.  
250 None of the models incorporate loss of surface microplastics from the open  
251 ocean by sinking or ingestion because there is insufficient data on these open-  
252 ocean loss rates. Furthermore, the models do not incorporate fragmentation and  
253 therefore treat particle count concentrations similar to mass concentrations.

254 The global microplastic distribution fields for the year 2014 from each of the  
255 three models were interpolated to a common 1° x 1° resolution and divided into  
256 six separate basins (the North and South Pacific, the North and South Atlantic,

257 the Indian, and the Mediterranean). For each basin and each model, the model  
258 prediction value was compared to the standardized plastic counts and mass at  
259 each of more than 11,000 locations. This yielded, for each basin and model, a  
260 regression coefficient used to scale the (unitless) model microplastics  
261 distribution to a solution of global microplastics abundance in units of particles  
262  $\text{km}^{-2}$  and  $\text{g km}^{-2}$ .

263

### 264 **3. Results**

265 The best-fitting GAM for the data standardization includes a two-dimensional  
266 spatial spline, a year term, first and second order terms for wind speed, and a  
267 discontinuity at the Americas between the Caribbean and Pacific basins (Table  
268 1). The region between the Caribbean and Pacific basins was the only portion of  
269 the sampling space where the number of samples and their proximity required  
270 incorporation of a spatial discontinuity, based on examination of the residuals  
271 from the model. The distance of the net tow was not a significant source of  
272 variability in the samples. Based on deviance, the final model explains 71.6% of  
273 the variation in observed plastic counts. The coefficient for sampling year is  
274 positive and significant, indicating increasing plastic concentrations over time.  
275 The wind terms indicate a negative but asymptotic relationship between plastic  
276 concentrations and wind speed (Table 1). The coefficient for the discontinuity at  
277 the Americas is not significant; however, based on AIC scores it significantly  
278 improved the model fit to the data and is therefore included.

279 In the standardized data, surface microplastic counts and mass varies by several  
280 orders of magnitude (Figure 1). The highest concentrations are in the centers of  
281 the subtropical gyres, mainly in the North Atlantic and North Pacific, where  
282 plastic particles accumulate due to convergence of Ekman transports (Kubota  
283 1994, van Sebille 2015). Concentrations are much lower in the tropics, poleward  
284 of 45°S and 45°N, and in the remote coastline off western Australia (Reisser *et al*  
285 2013). Microplastic counts and mass have similar patterns, although counts  
286 yield a ‘smoother’ field, especially in the Southern Hemisphere.

287 The three ocean circulation models scaled with the standardized data (hereafter  
288 “model solutions”) reasonably demonstrate the large variability in microplastic  
289 concentrations, and accurately capture the highest values ( $> \sim 10^5$  particles  $\text{km}^{-2}$ ,  
290 Figure 2a). However, the observed microplastic concentrations are much higher  
291 than the model solutions for concentrations below  $10^4$  particles  $\text{km}^{-2}$ . This bias  
292 could result from the detection limit in surface trawls; the lowest observable  
293 microplastic concentration above zero is 1 piece per trawl, which is equivalent  
294 to 540 particles  $\text{km}^{-2}$  for a typical surface trawl of 1 nautical mile (van Franeker  
295 and Law 2015). The standardization typically increases these values (Figure S2),  
296 enhancing the bias. In contrast, the models have no such limit and can reach  
297 much lower non-zero values. Beyond this obvious discrepancy between  
298 solutions and observations, there is a mismatch in the North Atlantic, where all  
299 models predict the highest concentrations around 60°W (Figure 3), whereas the  
300 highest observed concentrations are farther east (Figure 1).

301 The Van Sebille solution is skewed high compared to the other models,  
302 especially at very low concentrations (Figure 2b). This appears to be related to

303 the source function of the Van Sebille model, where microplastics are  
304 continuously released on an exponential growth curve, resulting in high  
305 concentrations even in regions of strong divergence. The skewedness disappears  
306 when the Van Sebille model is rerun with a one-time release of microplastics  
307 (Figure S3), although the Lebreton model also has an increasing source function  
308 over time.

309 The microplastic count and mass patterns broadly agree across model solutions  
310 (Figure 3), with all three showing high values in the subtropics and low values in  
311 the tropics and high latitudes. There are regional differences in high  
312 concentration areas such as the South Pacific, where the Maximenko solution  
313 has lower concentrations, and the North Atlantic, where the Lebreton solution  
314 has lower concentrations. In the Indian Ocean the Lebreton solution has lower  
315 concentrations and also has peak concentrations in the eastern rather than  
316 western basin like the other two models.

317 The largest differences between the three solutions occur in low concentration  
318 regions, visualized by calculating the ratio between highest and lowest solutions  
319 (in counts) at each point (Figure 4). Solutions differ by more than a factor of 100  
320 in the tropics and at high latitudes, whereas solutions in the centers of the  
321 accumulation zones differ by less than a factor of 10. The solutions also differ  
322 strongly in the Mediterranean, where the Lebreton and Van Sebille models  
323 project very high microplastic concentrations in the eastern basin, in contrast to  
324 the coarse-resolution ( $1/2^\circ$ ) Maximenko model, which was not designed for such  
325 small basins.

326 One reason for the discrepancies between model solutions could be the source  
327 function, which is continuous in time and non-uniformly distributed in space in  
328 the Van Sebille and Lebreton models, compared to the single initial release of  
329 evenly distributed microplastic in the Maximenko model. This might also explain  
330 the much lower concentrations near Asian coastlines and in the Mediterranean  
331 in the Maximenko solution. Another difference is the intra-annual variation in  
332 the statistics of ocean currents that is not accounted for in the Maximenko  
333 model, which could distort diffusion of particles from the high concentration  
334 gyres.

335 The three different model solutions can be aggregated by basin to yield total  
336 microplastic counts and mass (Figure 5, Tables 2 and 3), with black error bars  
337 representing the 95% confidence interval (see section 2.2) and grey error bars  
338 representing the 95% confidence interval of both the standardization procedure  
339 and the linear regression. For most basins the error bars are as large as, or larger  
340 than, the differences between the three solutions, with the North Atlantic and  
341 Mediterranean as exceptions.

342 The highest microplastic counts are in the Mediterranean (two solutions) and  
343 the North Pacific, while the largest microplastic mass is in the North Pacific in all  
344 three solutions. The total mass in the Mediterranean is much smaller because of  
345 the very small average particle mass and much smaller basin size. Surprisingly,  
346 the North Atlantic has low microplastic counts in all three solutions, and the  
347 lowest count and mass of any basin in the Lebreton model. This likely results  
348 from the relatively poor correlations between solutions and observations for

349 this basin (Figure 2), where the models do not achieve high enough  
350 concentrations in the center of the gyre.

351 The patterns of the basin-summed microplastic abundances in the three models  
352 are consistent with the basin-summed estimated total plastic waste available to  
353 enter the ocean in 2010 from Jambeck *et al* (2015), which was used as a source  
354 function in the Van Sebille model, but not in the other two models. With the  
355 exception of the Indian Ocean, the basin-summed microplastic mass is on the  
356 order of 1% of the estimated amount of plastic waste available to enter each  
357 basin in 2010. The smaller fraction in the Indian Ocean may be due to that basin  
358 being the most 'leaky', with a microplastic residence time of only a few years  
359 (van Sebille *et al* 2012).

360 The three solutions can be used to investigate the global abundance and  
361 distribution of microplastics (Tables 2 and 3). The Van Sebille model yields the  
362 highest total microplastic concentration ( $51.2 \times 10^{12}$  particles) and mass (236  
363 thousand metric tons), followed by the Lebreton model ( $31.2 \times 10^{12}$  particles,  
364 152 thousand metric tons) and the Maximenko model ( $14.9 \times 10^{12}$  particles, 93.3  
365 thousand metric tons). The Lebreton and Van Sebille estimates are not different  
366 at the 95% confidence interval (bars in Figure 6), while the Maximenko estimate  
367 is significantly lower, likely because of the single particle release combined with  
368 particle removal at coastlines. Even the lowest of the model solutions is  
369 substantially larger than the global microplastics estimates by Cózar *et al* (2014)  
370 (7 thousand to 35 thousand tons) and Eriksen *et al* (2014) ( $5.25 \times 10^{12}$  particles,  
371 66.1 thousand metric tons for particle sizes up to 200 mm).



372 The highest concentration of microplastics in any solution is  $10^8$  particles  $\text{km}^{-2}$   
373 in subtropical gyres, yet median concentrations range from  $4 \times 10^5$  particles  $\text{km}^{-2}$   
374 (Maximenko solution) to  $2 \times 10^6$  particles  $\text{km}^{-2}$  (Van Sebille solution) (Figure 6).  
375 This implies that 50% of microplastics are in relatively low concentration  
376 regions. For example, if accumulation zones are defined by microplastic  
377 concentrations greater than  $10^6$  particles  $\text{km}^{-2}$ , then between 30% (Lebreton  
378 solution) and 70% (Maximenko solution) of the microplastic resides *outside*  
379 these zones.

380 The solutions are dependent in part on the distribution of observational data. In  
381 all basins surface trawls tend to be clustered in relatively small regions, mostly  
382 in the accumulation zones themselves (Figure 1); thus, the regression between  
383 observations and model fields is biased towards agreement in these high  
384 concentration areas. To mitigate this effect we also computed solutions by fitting  
385 to observations inversely weighted by the number of observations in each grid  
386 cell, thereby putting more emphasis on observations in less-sampled areas. The  
387 resulting total microplastic counts and mass (Figure S4) show the same general  
388 pattern, but are slightly lower than the unweighted version and have slightly  
389 smaller error bars (Table S2). The exception is the Maximenko solution for mass,  
390 which increases slightly.

391

#### 392 **4. Discussion and Conclusions**

393 A major objective of this analysis is to inform the abundance and distribution of  
394 plastic debris in the ocean in order to ultimately assess marine animals'

395 exposure to and impact from interaction with debris. Ours is the third study to  
396 estimate the amount and distribution of small floating plastic particles in the  
397 global ocean, using the largest dataset to date and three different ocean  
398 circulation models. While the previous two studies found coarse agreement in  
399 the global mass of plastics collected using surface-trawling plankton nets (7-35  
400 thousand tons by C3zar *et al* 2014; 66 thousand metric tons by Eriksen *et al*  
401 2014), our model solutions not only exceed these but also vary substantially  
402 from 93 to 236 thousand metric tons.

403 Despite the wide discrepancy in these standing stock estimates, all analyses find  
404 the highest concentrations of net-collected plastics in the subtropical gyres, with  
405 the largest mass reservoir in the North Pacific Ocean, presumably because of its  
406 vast area and also the large inputs of plastic waste from coastlines of Asia and  
407 the United States (Jambeck *et al* 2015).

408 To a considerable extent, our mass estimates may be larger than previously  
409 published estimates because of the data standardization used. Adjusting each  
410 observation forward in time to a common sampling year of 2014 and to no-wind  
411 sampling conditions increased the observed plastic concentrations in nearly all  
412 samples (Fig S2). Previous studies have taken vertical wind-mixing of buoyant  
413 plastic debris into account by employing a simple one-dimensional model  
414 (Kukulka *et al* 2012) whose dynamics capture only a fraction of deep mixing  
415 observed (Brunner *et al* 2015). Certainly the variation in data collection (e.g., net  
416 mesh size); sample analysis (e.g., visual versus microscope identification); count-  
417 to-mass conversions (which are strongly dependent on particle size); and model

418 design (e.g., source functions and removal processes) also contribute to the  
419 discrepancies.

420 The variation in model solutions in our study emphasizes that most of the ocean  
421 surface is undersampled for microplastics. Uncertainties in the Southern  
422 Hemisphere basins illustrate the lack of data even in high concentration  
423 subtropical gyres. The least sampled regions are areas of low plastic  
424 concentrations, where models predict between 30% and 70% of particles may  
425 reside (Fig. 6). Perhaps the starkest illustration is in the Mediterranean Sea,  
426 where models predict between 21% and 54% of global microplastic particles,  
427 equivalent to between 5% and 10% of global mass (because of small average  
428 particle size), are located. Our dataset has only 105 surface trawls concentrated  
429 in a very small region of the western basin, whereas models predict the highest  
430 concentrations in the eastern basin. One might expect to find very large plastic  
431 concentrations given the predicted large inputs of land-based plastic waste  
432 (Jambeck *et al* 2015) and the very long residence time of surface waters due to  
433 lack of exchange with the North Atlantic. Indeed, recent field data not included in  
434 this study confirmed very high mean surface concentrations in the southern  
435 Adriatic Sea from 29 surface trawls (1.05 million particles km<sup>-2</sup>; 442 g km<sup>-2</sup>;  
436 (Suaria *et al* 2015)), yet more data, especially in the eastern basin, is strongly  
437 needed.

438 Any global estimate of total accumulated floating microplastic debris is only on  
439 order of 1% or less of the amount of plastic waste available to enter the ocean  
440 annually from land-based sources. While these source estimates from Jambeck *et*  
441 *al* (2015) have relatively large uncertainties themselves (for example because

442 they omit the tonnage of plastic locally burned, buried and recovered by self-  
443 employed wastepickers), it is hard to see their source and our floating stock  
444 estimates converge. While some of the 'missing' mass would be in plastic items  
445 larger than 200 mm (e.g. Eriksen *et al* 2014), and hence not included in our  
446 study, this is unlikely to account for the two orders of magnitude difference.

447 Importantly, however, there is no reason that standing stock estimates should  
448 equal an annual input estimate, especially since the input is of all plastic  
449 materials, not just those that float. Seafloor deposits of dense plastics, coastal  
450 deposits, and debris larger than typically captured in plankton nets are  
451 undoubtedly important reservoirs of plastic debris. In addition, standing stock  
452 reflects inputs and removal over time. The input rate is a function of not only the  
453 amount of plastic entering the ocean, but also of the rate at which these  
454 presumably large items fragment into the microplastics that surface trawls  
455 mostly collect. Removal processes are hypothesized (Law *et al* 2010), but their  
456 rates are essentially unknown. Multi-decadal time series of industrial resin  
457 pellets in the North Atlantic subtropical gyre and in North Sea seabirds indicate  
458 that removal can be quite rapid (van Franeker and Law 2015). Microplastics  
459 might fragment to as-yet undetectable sizes, sink due to buoyancy loss (Ye and  
460 Andrady 1991), be deposited on shorelines (McDermid and McMullen 2004), or  
461 be ingested and subsequently reduced in size (e.g., due to digestive grinding)  
462 and/or transported to land or the seafloor upon egestion. Biota represent the  
463 only other reservoir for which microplastic mass estimates exist. Myctophid  
464 fishes in the North Pacific gyre were estimated to hold 12 to 24 thousand metric  
465 tons of microplastic (Davison and Asch 2011), and the growing knowledge on

466 ingestion of plastics by fishes (Kühn *et al* 2015) could imply a reservoir  
467 comparable in size to the sea surface.

468 The order-of-magnitude discrepancies in these global-scale budgeting exercises  
469 reveal a fundamental gap in understanding akin to the “missing” anthropogenic  
470 carbon dioxide in the carbon budgeting exercise of the early 2000s (e.g.  
471 Stephens *et al* 2007). Until these discrepancies are resolved at even a coarse  
472 scale, we cannot quantify the full suite of impacts of plastic debris on the marine  
473 ecosystem.

474

## 475 **Acknowledgements**

476 This work was conducted within the Marine Debris Working Group at the  
477 National Center for Ecological Analysis and Synthesis, University of California,  
478 Santa Barbara, with support from Ocean Conservancy. We particularly thank  
479 George Leonard and Nick Mallos for their support, and Steven D. Gaines for  
480 thoughtful insights. We thank H. Carson, A. Cózar, M. Doyle, C. Fossi, G. Lattin, C.  
481 Panti, R. Yamashita, and A. Zellers for kind assistance in compiling plankton net  
482 data. EvS was supported by the Australian Research Council (DE130101336).  
483 BDH and CW were supported by CSIRO’s Oceans and Atmosphere Flagship. JAF  
484 was supported by IMARES internal funds. NM was partly supported by NASA  
485 through grants NNX08AR49G and NNX13AK35G. IPRC/SOEST Publication  
486 XXX/XXXX. KLL was supported by the National Science Foundation (OCE-  
487 1260403) and Sea Education Association. We thank two anonymous reviewers  
488 for their helpful comments.

489 **References:**

- 490 Barnes D K A, Galgani F, Thompson R C and Barlaz M A 2009 Accumulation and  
491 fragmentation of plastic debris in global environments *Phil Trans R Soc B*  
492 **364** 1985–98
- 493 Brunner K, Kukulka T, Proskurowski G and Law K L 2015 Passive buoyant  
494 tracers in the ocean surface boundary layer: II. Observations and simulations  
495 of microplastics marine debris *J Geophys Res* **submitted**
- 496 Buckland S, Anderson D R, Burnham K P, J L, Borchers D and Thomas L 2001  
497 *Introduction to Distance Sampling: Estimating Abundance of*  
498 *Biological Populations* (Oxford: Oxford University Press)
- 499 Cózar A, Echevarría F, González-Gordillo J I, Irigoien X, Ubeda B, Hernández-León  
500 S, Palma Á T, Navarro S, García-de-Lomas J, Ruiz A, Fernández-de-Puelles M L  
501 and Duarte C M 2014 Plastic debris in the open ocean *Proc Natl Acad Sci* **111**  
502 10239–44
- 503 Davison P and Asch R G 2011 Plastic ingestion by mesopelagic fishes in the  
504 North Pacific Subtropical Gyre *Marine Ecology-Progress Series* **432** 173–80
- 505 Dee D P, Uppala S M, Simmons A J, Berrisford P, Poli P, Kobayashi S, Andrae U,  
506 Balmaseda M A, Balsamo G, Bauer P, Bechtold P, Beljaars A C M, van de Berg  
507 L, Bidlot J, Bormann N, Delsol C, Dragani R, Fuentes M, Geer A J, Haimberger  
508 L, Healy S B, Hersbach H, Hólm E V, Isaksen L, Kállberg P, Köhler M,  
509 Matricardi M, McNally A P, Monge-Sanz B M, Morcrette J J, Park B K, Peubey  
510 C, de Rosnay P, Tavolato C, Thépaut J N and Vitart F 2011 The ERA-Interim  
511 reanalysis: configuration and performance of the data assimilation system *Q*  
512 *J Roy Meteor Soc* **137** 553–97
- 513 Eriksen M, Lebreton L C M, Carson H S, Thiel M, Moore C J, Borerro J C, Galgani F,  
514 Ryan P G and Reisser J 2014 Plastic Pollution in the World's Oceans: More  
515 than 5 Trillion Plastic Pieces Weighing over 250,000 Tons Afloat at Sea *PLOS*  
516 *One* **9** e111913
- 517 Eriksen M, Maximenko N A, Thiel M, Cummins A, Lattin G, Wilson S, Hafner J,  
518 Zellers A F and Rifman S 2013 Plastic pollution in the South Pacific  
519 subtropical gyre *Mar Pollut Bull* **68** 71–6
- 520 Goldstein M C, Rosenberg M and Cheng L 2012 Increased oceanic microplastic  
521 debris enhances oviposition in an endemic pelagic insect *Biol Lett* **8** 817–20
- 522 Jambeck J R, Geyer R, Wilcox C, Siegler T R, Perryman M, Andrady A L, Narayan R  
523 and Law K L 2015 Plastic waste inputs from land into the ocean *Science* **347**  
524 768–71
- 525 Kubota M 1994 A mechanism for the accumulation of floating marine debris  
526 north of Hawaii *J Phys Oceanogr* **24** 1059–64
- 527 Kukulka T, Proskurowski G, Morét-Ferguson S E, Meyer D W and Law K L 2012

- 528 The effect of wind mixing on the vertical distribution of buoyant plastic  
529 debris *Geophysical Research Letters* **39** L07601–n/a
- 530 Kühn S, Bravo Rebolledo E L and van Franeker J A 2015 Deleterious Effects of  
531 Litter on Marine Life *Deleterious Effects of Litter on Marine Life* ed M  
532 Bergmann, L Gutow and M Klages (Cham: Springer International Publishing)  
533 pp 75–116
- 534 Law K L, Morét-Ferguson S E, Goodwin D S, Zettler E R, DeForce E, Kukulka T and  
535 Proskurowski G 2014 Distribution of Surface Plastic Debris in the Eastern  
536 Pacific Ocean from an 11-Year Data Set *Environ Sci Technol* **48** 4732–8
- 537 Law K L, Morét-Ferguson S E, Maximenko N A, Proskurowski G, Peacock E E,  
538 Hafner J and Reddy C M 2010 Plastic accumulation in the North Atlantic  
539 subtropical gyre *Science* **329** 1185–8
- 540 Lebreton L C M, Greer S D and Borerro J C 2012 Numerical modelling of floating  
541 debris in the world's oceans *Mar Pollut Bull* **64** 653–61
- 542 Maximenko N A, Hafner J and Niiler P P 2012 Pathways of marine debris derived  
543 from trajectories of Lagrangian drifters *Mar Pollut Bull* **65** 51–62
- 544 McDermid K J and McMullen T L 2004 Quantitative analysis of small-plastic  
545 debris on beaches in the Hawaiian archipelago *Mar Pollut Bull* **48** 790–4
- 546 Morét-Ferguson S E, Law K L, Proskurowski G, Murphy E K, Peacock E E and  
547 Reddy C M 2010 The size, mass, and composition of plastic debris in the  
548 western North Atlantic Ocean *Mar Pollut Bull* **60** 1873–8
- 549 Obbard R W, Sadri S, Wong Y Q, Khitun A A, Baker I and Thompson R C 2014  
550 Global warming releases microplastic legacy frozen in Arctic Sea ice *Earth's*  
551 *Future* **2** 315–20
- 552 Plastics Europe 2013 *Plastics – the Facts 2013: An analysis of European latest*  
553 *plastics production, demand and waste data* (Brussels: Plastics Europe)
- 554 Plastinum 2009 Plastic Industry and Recycling  
555 [http://www.plastinum.com/plastinum/Plastic-Industry-Recycling/The-](http://www.plastinum.com/plastinum/Plastic-Industry-Recycling/The-global-plastics-industry-continued-growth)  
556 [global-plastics-industry-continued-growth](http://www.plastinum.com/plastinum/Plastic-Industry-Recycling/The-global-plastics-industry-continued-growth)
- 557 Reisser J, Shaw J, Wilcox C, Hardesty B D, Proietti M, Thums M and Pattiaratchi C  
558 2013 Marine Plastic Pollution in Waters around Australia: Characteristics,  
559 Concentrations, and Pathways ed G C Hays *PLOS One* **8** e80466
- 560 Reisser J, Slat B, Noble K, Plessis du K, Epp M, Proietti M, de Sonnevile J, Becker  
561 T and Pattiaratchi C 2015 The vertical distribution of buoyant plastics at sea:  
562 an observational study in the North Atlantic Gyre *Biogeosciences* **12** 1249–56
- 563 Rochman C M, Browne M A, Underwood A J, van Franeker J A and Thompson R C  
564 2015 The ecological impacts of marine debris: unraveling the demonstrated  
565 evidence from what is perceived *Ecol*

- 566 Ryan P G 2013 A simple technique for counting marine debris at sea reveals  
567 steep litter gradients between the Straits of Malacca and the Bay of Bengal  
568 *Mar Pollut Bull* **69** 128–36
- 569 Schlining K, Thun von S, Kuhnz L, Schlining B, Lundsten L, Stout N J, Chaney L  
570 and Connor J 2013 Debris in the deep: Using a 22-year video annotation  
571 database to survey marine litter in Monterey Canyon, central California, USA  
572 *Deep-Sea Research Part I* **79** 96–105
- 573 Stephens B B, Gurney K R, Tans P P, Sweeney C, Peters W, Bruhwiler L, Ciais P,  
574 Ramonet M, Bousquet P, Nakazawa T, Aoki S, Machida T, Inoue G,  
575 Vinnichenko N, Lloyd J, Jordan A, Heimann M, Shibistova O, Langenfelds R L,  
576 Steele L P, Francey R J and Denning A S 2007 Weak northern and strong  
577 tropical land carbon uptake from vertical profiles of atmospheric CO<sub>2</sub>  
578 *Science* **316** 1732–5
- 579 Suaria G, Avio C, Lattin G and Aliani S 2015 Neustonic microplastics in the  
580 Southern Adriatic Sea. Preliminary results. *Micro* 2015 p 42
- 581 Thompson R C, Olsen Y, Mitchell R P, Davis A, Rowland S J, John A, McGonigle D  
582 and Russell A E 2004 Lost at sea: Where is all the plastic? *Science* **304** 838–8
- 583 van Franeker J A and Law K L 2015 Seabirds, gyres and global trends in plastic  
584 pollution *Environmental Pollution* **203** 89–96
- 585 van Sebille E 2014 Adrift.org.au — A free, quick and easy tool to quantitatively  
586 study planktonic surface drift in the global ocean *J Exp Mar Biol Ecol* **461**  
587 317–22
- 588 van Sebille E 2015 The oceans' accumulating plastic garbage *Physics Today* **68**  
589 60–1
- 590 van Sebille E, England M H and Froyland G 2012 Origin, dynamics and evolution  
591 of ocean garbage patches from observed surface drifters *Environ Res Lett* **7**  
592 044040
- 593 Williams R, O'Hara P D and Ashe E 2011 Marine mammals and debris in coastal  
594 waters of British Columbia, Canada *Mar Pollut Bull* **62** 1303–16
- 595 Wood S N 2006 *Generalized additive models: an introduction with R* (Boca Raton,  
596 Florida, USA: Chapman Hall/CRC)
- 597 Woodall L C, Sanchez-Vidal A, Canals M, Paterson G L J, Coppock R, Sleight V,  
598 Calafat A, Rogers A D, Narayanaswamy B E and Thompson R C 2014 The  
599 deep sea is a major sink for microplastic debris *Royal Society Open Science* **1**  
600 140317–7
- 601 Ye Y and Andrady A L 1991 Fouling of Floating Plastic Debris Under Biscayne  
602 Bay Exposure Conditions *Mar Pollut Bull* **22** 608–13

603



604  
605

**Tables**

| A. Model Fit |          | B. Best Fit Model Coefficients      |          |         |                        |
|--------------|----------|-------------------------------------|----------|---------|------------------------|
| Model        | AIC      | Coefficient                         | Estimate | std err | p value                |
| SAyWWsqBd2   | 159533.3 | Intercept                           | 7.3      | 3.4     | 0.033                  |
| SAyWWsqBd    | 159537.7 | Year (since 1950)                   | 0.016    | 0.005   | 0.0012                 |
| SAyWWsq      | 159538.2 | Wind Speed                          | -0.34    | 0.045   | 1.40x10 <sup>-13</sup> |
| SAyWBd       | 159541.9 | Wind Speed Squared                  | 0.011    | 0.0044  | 0.015                  |
| SAyWBd2      | 159541.9 | Atlantic – Pacific Boundary Squared | 3.7      | 8.4     | 0.67                   |
| SAyW         | 159542.4 |                                     |          |         |                        |
| SWWsq        | 159592.8 |                                     |          |         |                        |
| SW           | 159598.4 |                                     |          |         |                        |
| SWsq         | 159727.7 |                                     |          |         |                        |
| S            | 160546.3 |                                     |          |         |                        |
| 0            | 177503.4 |                                     |          |         |                        |

606  
607  
608  
609  
610  
611  
612

**Table 1.** Adequacy of the candidate standardization models and coefficients of the best fitting model. Model codes in panel A are: 0 – intercept only, S – spherical smooth, W – wind speed, Wsq – wind speed squared, Bd – Caribbean–Pacific discontinuity, Bd2 - Caribbean–Pacific discontinuity squared, Ay – Sampling Year (since 1950). Lower AIC indicates an improved model, with a difference of 2 units suggesting statistically significant improvements.

| Count                           | Maximenko model |                             |                            | Lebreton model |                             |                            | Van Sebillé model |                             |                            |
|---------------------------------|-----------------|-----------------------------|----------------------------|----------------|-----------------------------|----------------------------|-------------------|-----------------------------|----------------------------|
|                                 | Best<br>Est     | <i>Stand</i><br><i>C.I.</i> | <i>Regr</i><br><i>C.I.</i> | Best<br>Est    | <i>Stand</i><br><i>C.I.</i> | <i>Regr</i><br><i>C.I.</i> | Best<br>Est       | <i>Stand</i><br><i>C.I.</i> | <i>Regr</i><br><i>C.I.</i> |
| [10 <sup>12</sup><br>particles] |                 |                             |                            |                |                             |                            |                   |                             |                            |
| <b>N Pac</b>                    | 7.3             | 1.2                         | 0.1                        | 9.4            | 1.7                         | 0.5                        | 15.9              | 2.7                         | 0.4                        |
| <b>S Pac</b>                    | 0.3             | 0.1                         | 0.0                        | 0.7            | 0.4                         | 0.1                        | 0.8               | 0.4                         | 0.0                        |
| <b>N Atl</b>                    | 0.4             | 0.1                         | 0.0                        | 0.3            | 0.1                         | 0.0                        | 1.3               | 0.3                         | 0.1                        |
| <b>S Atl</b>                    | 1.0             | 0.3                         | 0.2                        | 2.6            | 0.9                         | 0.3                        | 2.0               | 0.7                         | 0.1                        |
| <b>Ind</b>                      | 2.8             | 1.7                         | 0.3                        | 2.0            | 1.3                         | 0.5                        | 3.0               | 1.9                         | 0.6                        |
| <b>Med</b>                      | 3.2             | 0.5                         | 0.3                        | 16.1           | 2.5                         | 1.5                        | 28.2              | 4.4                         | 4.8                        |
| <b>Total</b>                    | 14.9            | 2.1                         | 0.5                        | 31.2           | 3.4                         | 1.7                        | 51.2              | 5.6                         | 4.9                        |

613

614 **Table 2:** Overview of the modeled microplastic count solutions per basin, in 10<sup>12</sup>  
615 particles. For each of the three models, the best estimates as well as the 95%  
616 confidence intervals related to both the standardization (*Stand C.I.*) and  
617 regression (*Regr C.I.*) are given.

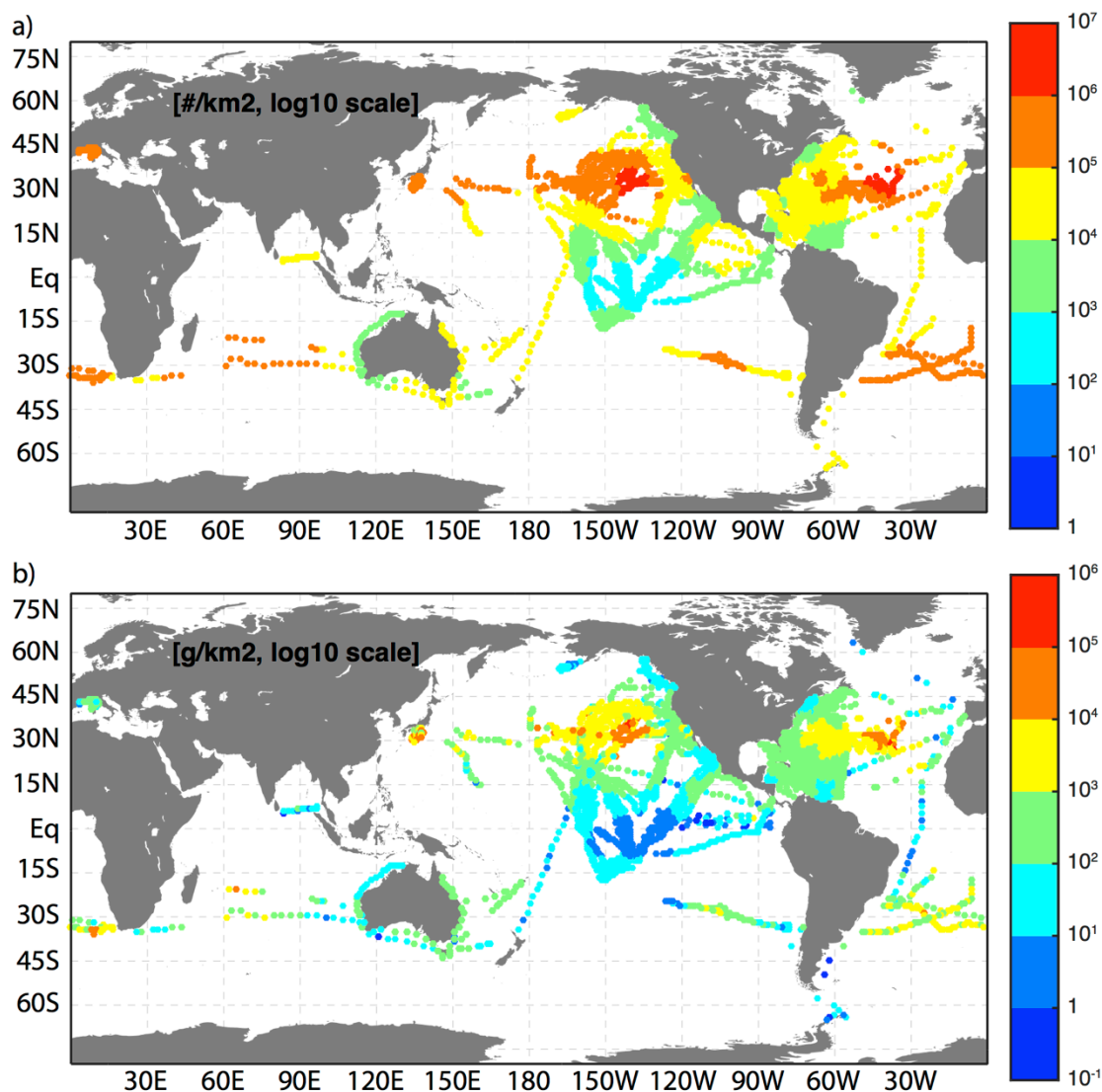
618

| Mass                         | Maximenko model |                             |                            | Lebreton model |                             |                            | Van Sebillé model |                             |                            |
|------------------------------|-----------------|-----------------------------|----------------------------|----------------|-----------------------------|----------------------------|-------------------|-----------------------------|----------------------------|
|                              | Best<br>Est     | <i>Stand</i><br><i>C.I.</i> | <i>Regr</i><br><i>C.I.</i> | Best<br>Est    | <i>Stand</i><br><i>C.I.</i> | <i>Regr</i><br><i>C.I.</i> | Best<br>Est       | <i>Stand</i><br><i>C.I.</i> | <i>Regr</i><br><i>C.I.</i> |
| [thousand<br>metric<br>tons] |                 |                             |                            |                |                             |                            |                   |                             |                            |
| <b>N Pac</b>                 | 62.8            | 10.9                        | 11.9                       | 108.2          | 20.7                        | 22.4                       | 155.2             | 28.0                        | 28.2                       |
| <b>S Pac</b>                 | 1.0             | 0.5                         | 0.1                        | 3.7            | 1.8                         | 0.4                        | 3.7               | 1.8                         | 0.3                        |
| <b>N Atl</b>                 | 5.1             | 1.1                         | 0.7                        | 3.6            | 0.8                         | 0.7                        | 17.7              | 3.8                         | 1.6                        |
| <b>S Atl</b>                 | 6.2             | 2.1                         | 2.5                        | 15.5           | 5.4                         | 5.8                        | 14.2              | 5.0                         | 3.6                        |
| <b>Ind</b>                   | 13.3            | 8.3                         | 6.6                        | 5.5            | 3.5                         | 7.5                        | 15.0              | 9.6                         | 8.4                        |
| <b>Med</b>                   | 4.8             | 0.7                         | 1.6                        | 15.0           | 2.3                         | 5.9                        | 30.3              | 4.9                         | 11.9                       |
| <b>Total</b>                 | 93.3            | 13.9                        | 14.0                       | 151.5          | 21.9                        | 25.0                       | 236.0             | 30.7                        | 32.0                       |

619

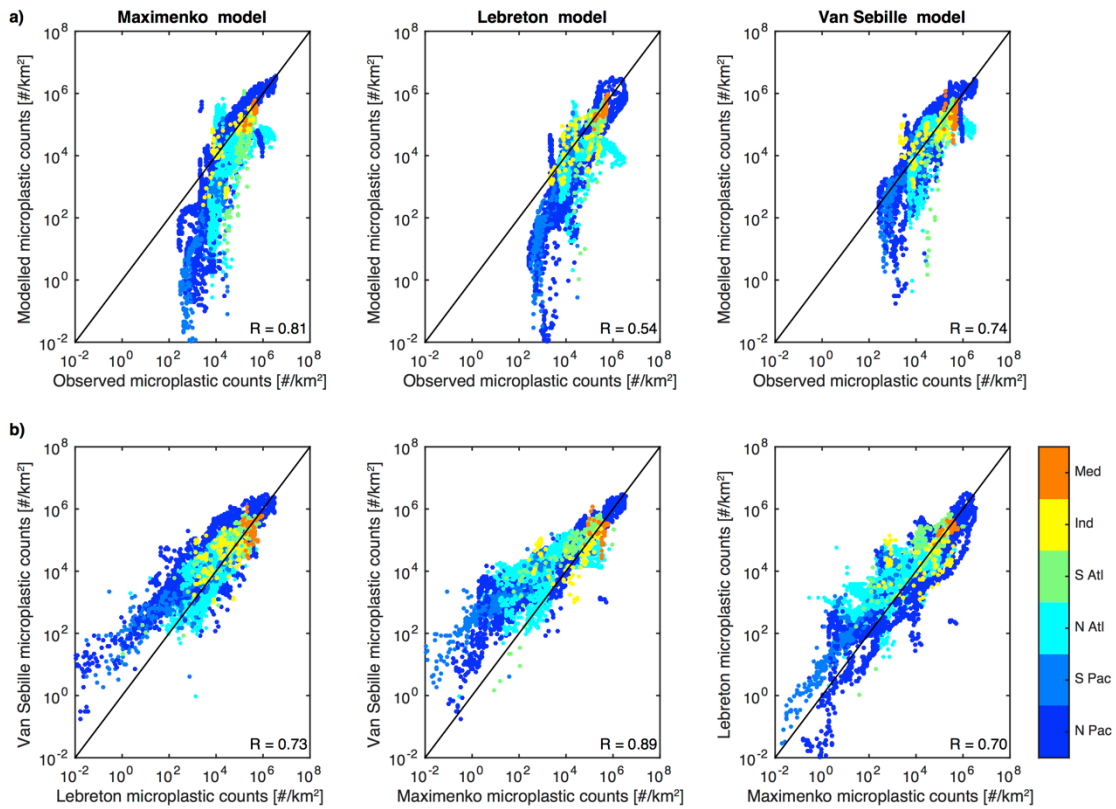
620 **Table 3:** Overview of the modeled microplastic mass solutions per basin, in  
621 thousand metric tons. For each of the three models, the best estimates as well as  
622 the 95% confidence intervals related to both the standardization (*Stand C.I.*) and  
623 regression (*Regr C.I.*) are given.

624 **Figures**



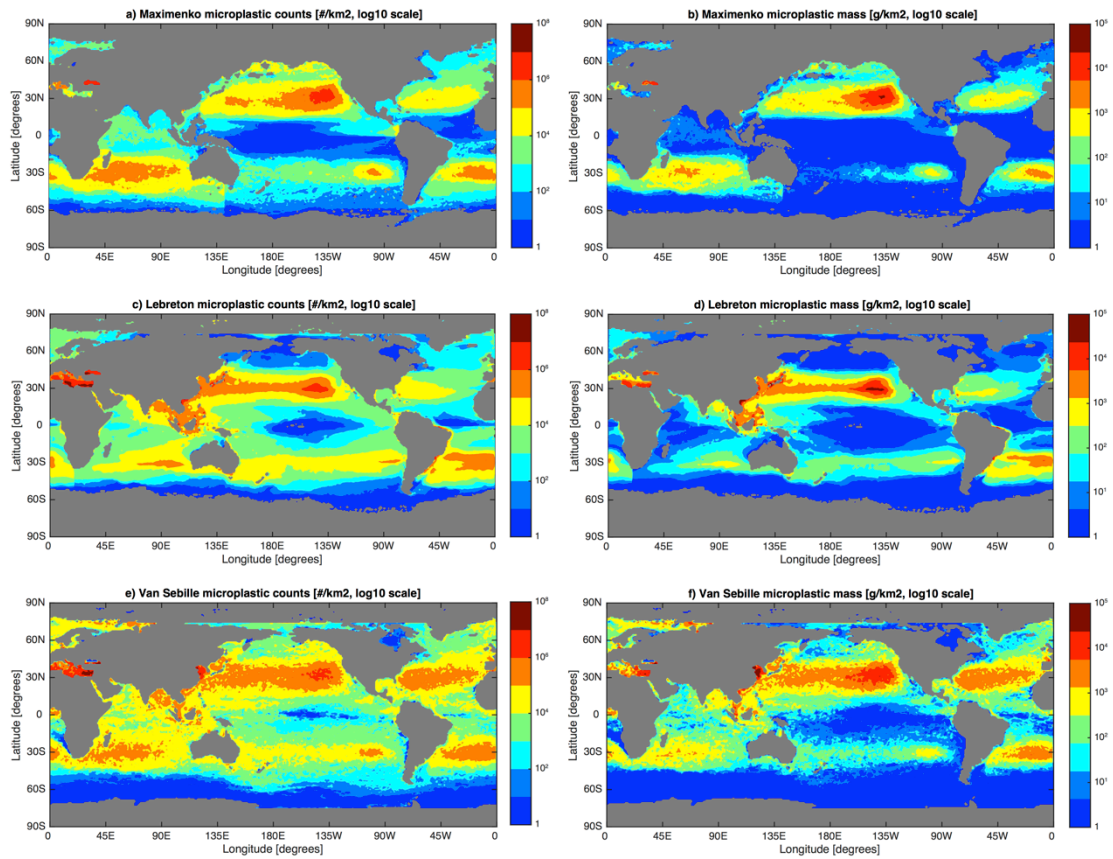
625

626 **Figure 1:** The location and standardized (a) microplastic count and (b)  
627 microplastic mass of all surface trawl data used in this analysis, on a log10 scale.  
628 Standardization is done with respect to year of study, geographic location, and  
629 wind speed. The spatial term includes a discontinuity at the Americas to allow  
630 for differences between the Caribbean Sea and tropical Pacific Ocean. Compare  
631 to Figure S1 for the raw, un-standardized data.



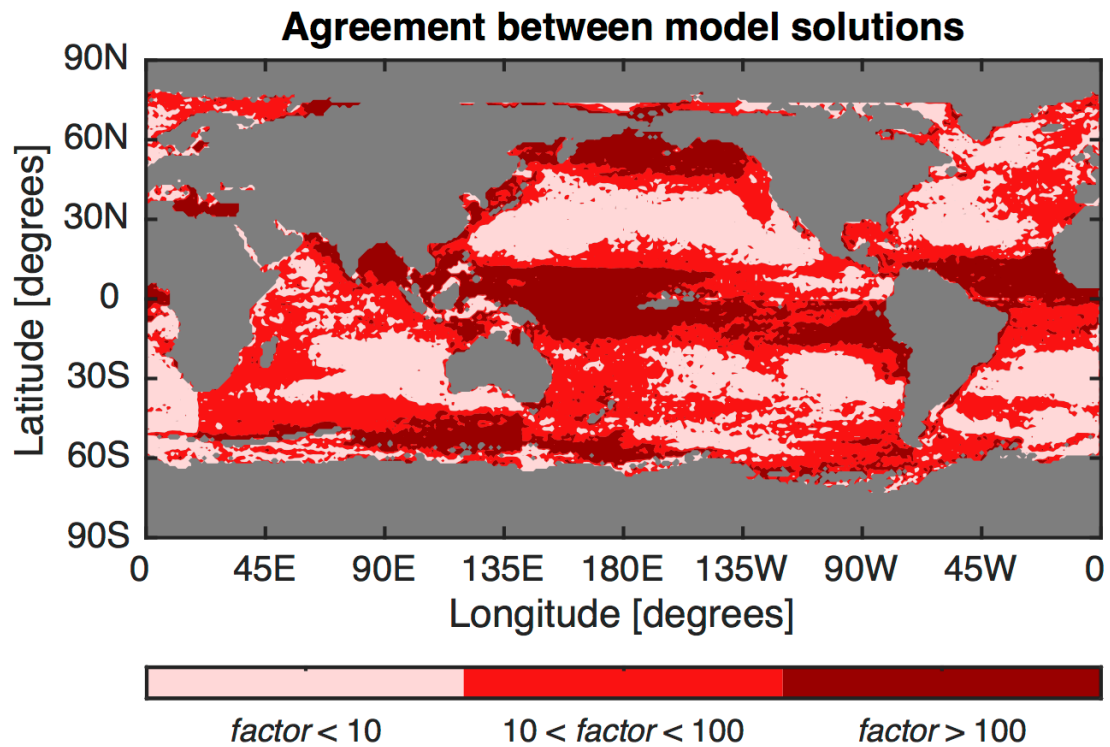
632

633 **Figure 2:** a) Comparison between the three ocean models and the standardized  
 634 observations (top row), and b) inter-comparison between the three ocean  
 635 models (bottom row), at each surface trawl location. The points are color coded  
 636 according to basin, and the black lines are the one-to-one lines. The correlations  
 637 reported in the top row give an estimate of agreement between the models and  
 638 observations. All models reach much lower microplastic counts than the  
 639 observations, likely because of detection limits of surface trawls (see text). The  
 640 Van Sebille model gives slightly higher values than the other two models,  
 641 particularly for regions where microplastic counts are low.



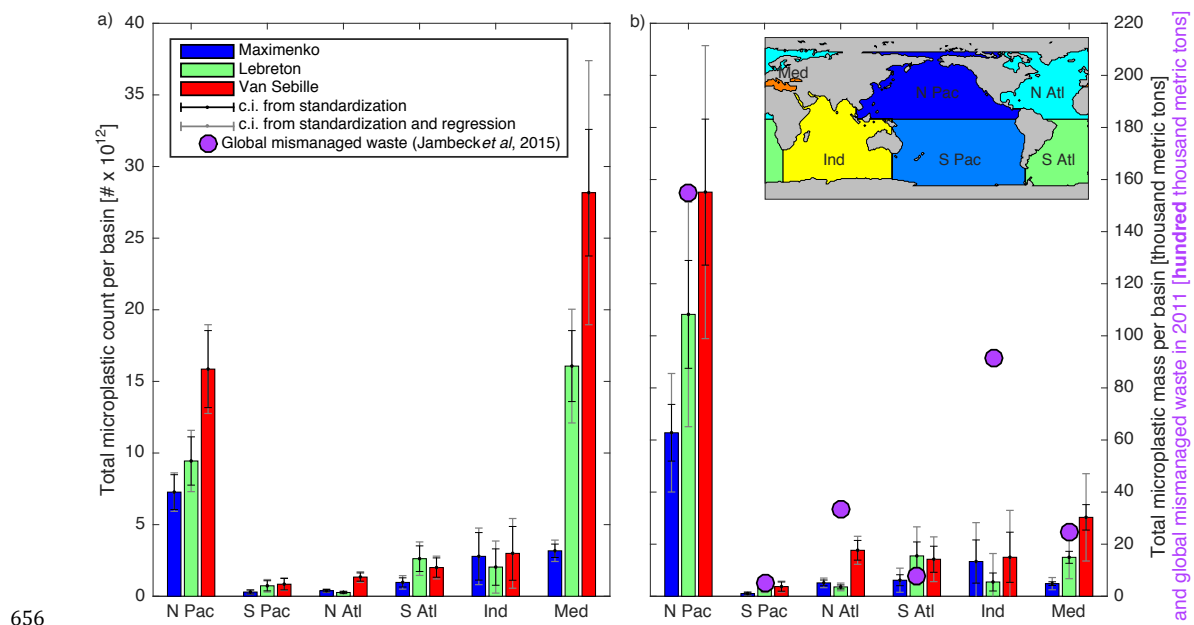
642

643 **Figure 3:** Maps of the solutions of microplastic count (left column) and mass  
 644 (right column) distribution for the three different models. Because fits are done  
 645 on a per-basin level, there are a few discontinuities visible (e.g. south of  
 646 Tasmania in the Maximenko solution, panel a).

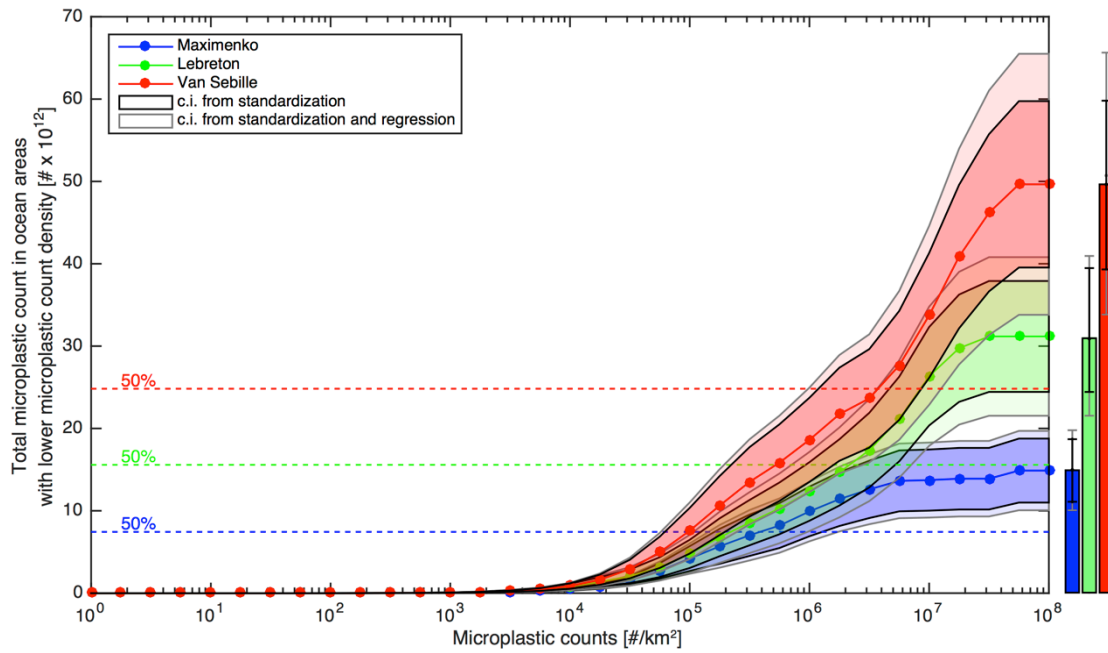


647

648 **Figure 4:** Map showing the level of agreement between the three different  
 649 models, in terms of microplastic counts. Pink shading denotes areas where the  
 650 lowest and highest estimates differ by less than a factor of 10; red shading  
 651 denotes areas where the lowest and highest estimates differ by between a factor  
 652 of 10 and 100; and dark red shading denotes areas where the lowest and highest  
 653 estimates differ by more than a factor of 100. The three models agree reasonably  
 654 well within the centers of the gyres, but strongly differ in the tropics, the high  
 655 latitudes, and the eastern Mediterranean.



657 **Figure 5:** Bar plot of (a) the total amount of microplastic particles in each of the  
 658 basins and (b) the total mass of microplastics in each of the basins in units of  
 659 thousand metric tons, for the three different model solutions for 2014. Error  
 660 bars indicate 95% confidence intervals, with the black bars the error due to the  
 661 standardization, and the grey bars the error due to the standardization and the  
 662 linear regression. The purple dots in (b) are the basin-summed estimates of the  
 663 amount of plastic waste available to enter the ocean in 2010 (Jambeck *et al*  
 664 2015), in units of hundred thousand metric tons (note scale difference from total  
 665 microplastic mass). All models predict the largest microplastic mass in the North  
 666 Pacific Ocean. While there are a large number of particles in the Mediterranean  
 667 basin (in the Lebreton and Van Sebille model), they have a very small average  
 668 mass (Table S1) and therefore do not account for much of the total mass. The  
 669 largest differences between the models are in the Mediterranean Sea, and to a  
 670 lesser extent in the North Pacific and Atlantic basins. The models agree quite  
 671 well on the amount of microplastic particles in the Indian and South Pacific  
 672 basins.



673

674 **Figure 6:** Cumulative frequencies of microplastic concentrations, for the three  
 675 different model solutions. The shaded areas represent the 95% confidence  
 676 interval due to the standardization (darkest hues and black lines) and due to  
 677 both the standardization and the regression (lightest hues and grey lines). For  
 678 example, in the Lebreton solution, 50% of the microplastic is in regions of the  
 679 ocean where microplastic concentrations are lower than  $2 \times 10^6$  particles  $\text{km}^{-2}$ ,  
 680 whereas in the Maximenko solution 50% of the particles are in regions where  
 681 microplastic concentrations are lower than  $4 \times 10^5$  particles  $\text{km}^{-2}$ . Between 30%  
 682 (Lebreton) and 70% (Maximenko) of particles reside in regions of low  
 683 concentration ( $< 10^6$  particles  $\text{km}^{-2}$ ).